

Structural Studies of the Hemocyanin Active Site. 1. Extended X-ray Absorption Fine Structure (EXAFS) Analysis¹

J. M. Brown,^{2a,b} L. Powers,^{2c} B. Kincaid,^{2c} J. A. Larrabee,^{2a,b} and T. G. Spiro*^{2a}

Contributions from Bell Laboratories, Murray Hill, New Jersey 07974,
and the Department of Chemistry, Princeton University, Princeton, New Jersey 08540.
Received November 26, 1979

Abstract: X-ray absorption spectra near the Cu K edge have been obtained for oxy- and deoxyhemocyanin (Hc) from *Busycon canaliculatum* using synchrotron radiation. Comparison with copper complexes shows the edge structure to be consistent with imidazole coordination of Cu(II) and Cu(I), respectively. The Fourier transform of the extended fine structure (EXAFS) shows two well-defined peaks. The positions and shape of the first peaks require coordination by low-Z atoms only, at average distances of 1.96 and 1.95 Å for the copper atoms of oxy- and deoxyHc. Their coordination numbers are calculated to be four and two, respectively, but the uncertainties are large; five and three are considered to be likelier values on the basis of chemical and spectroscopic evidence. The outer Fourier peak places a backscattering atom at 3.7 and 3.4 Å from Cu in oxy- and deoxyHc. For oxyHc this atom is shown to be the other Cu by the shape of the retransformed amplitude function. For deoxyHc the outer shell peak can be fit either with Cu or with a first-row scatterer. In the latter case, however, neither the distance nor the required Debye-Waller factor is sensible chemically, and a Cu-Cu interaction is the preferred interpretation. These results, along with those from resonance Raman and electronic absorption spectroscopy, lead to a model of the Hc binding site. It has two Cu atoms bound to the protein via three histidine ligands each; in oxyHc the Cu(II) ions are bridged by the bound O₂²⁻ and by an atom from a protein ligand, possibly tyrosine.

Introduction

Hemocyanin (Hc), the oxygen-carrying protein of molluscs and arthropods,³⁻⁵ although colorless in its deoxy form, contains copper and binds one oxygen molecule per two copper atoms, with the generation of a blue color and a rich electronic spectrum.^{6,7} Resonance Raman studies in the visible region^{8,9} have established that the bound dioxygen O-O stretch is at a frequency, 744-749 cm⁻¹, characteristic of peroxide, implying essentially complete transfer of two electrons to O₂ on binding, and an active-site composition that can be formulated as Cu₂²⁺O₂²⁻, the deoxy form containing Cu⁺. The oxyprotein is not detectably paramagnetic,¹⁰⁻¹² however, indicating that the Cu²⁺ ions are antiferromagnetically coupled. With respect to the copper coordination group, an electron paramagnetic resonance (EPR) study of nitric oxide treated hemocyanin indicated at least two nitrogen ligands,¹³ and there is much chemical evidence for imidazole coordination.¹⁴⁻¹⁶ There is evidence against bound carboxylate,¹⁴ and both for^{7,15,17} and against^{18,19} bound tyrosine. Cysteine sulfur has also been suggested as a ligand,¹⁷ but runs counter to chemical²⁰ and photoelectron spectroscopic²¹ evidence.

Not only are these characteristics intriguing in and of themselves, but they bear on the general mechanism of dioxygen activation by metalloproteins. Tyrosinase, a copper-containing enzyme which utilizes dioxygen in the hydroxylation of monophenols and the dehydrogenation of ortho diphenols, has characteristics that are quite similar to those of hemocyanin,^{13,22-24} and UV resonance Raman spectroscopy has recently demonstrated that the binding site structure of oxytyrosinase from *Neurospora crassa* is essentially the same as that of oxyhemocyanin.²⁵ The copper-containing terminal oxidases, laccase and ceruloplasmin, also contain antiferromagnetically coupled Cu²⁺ pairs (type 3 copper), which may be at the oxygen binding site.²⁶ Finally, cytochrome oxidase, the dioxygen terminus of the mitochondrial electron transport chain, contains two copper atoms, although in this case one Cu²⁺ and one heme Fe³⁺ appear to be antiferromagnetically coupled²⁷ and may be involved in dioxygen binding.

Further structural characterization of the Hc binding site is clearly desirable. X-ray crystal-structure determinations are in progress^{28,29} but are hampered by the complexities of the

Hc subunit structure.^{29b} In this study and the succeeding one¹ we have studied the Hc active site using two independent and complementary physical techniques: extended X-ray absorption fine structure (EXAFS) and resonance Raman (RR) spectroscopy. EXAFS provides a method for probing the surroundings of an X-ray absorbing atom from the modulation of the absorptivity above the edge (K edge) due to the photoelectron backscattering from the surrounding atoms.^{30a}

The EXAFS absorptivity modulation depends directly on interatomic distances as:

$$\chi(k) = \sum_i \frac{-N_i |f_i(\pi, k)|}{k R_i^2} e^{-2R_i/\lambda} e^{-2\sigma_i^2 k^2} \times \sin(2kR_i + \alpha_i(k)) \quad (1)$$

where the sum runs over distinct distances R_i relative to the absorbing atom, N_i is the number of atoms of the same type at R_i , λ is the photoelectron mean free path, $f_i(\pi, k)$ is the i th atoms backscattering amplitude, σ_i^2 is the mean square displacement in R_i , and $\alpha_i(k)$ is an energy-dependent phase shift in the photoelectron wave introduced by the molecular potential. k , the magnitude of the photoelectron wavevector, is given by:

$$k = (2m_e(E - E_0))^{1/2}/\hbar \quad (2)$$

where m_e is the electron mass and E_0 is the threshold energy. Analysis of the EXAFS can thus provide information about the radial distribution of atoms around the X-ray absorber. In addition, the structure of the edge itself, reflecting electronic transitions to bound states below the dissociation limit, can sometimes provide information about the oxidation and chemical state of the absorber. EXAFS has been applied to the determination of bond lengths and neighboring atom types and numbers in iron-sulfur proteins,^{31a,b} heme proteins,³² molybdenum-containing proteins,^{33a,b,c} copper proteins,^{33d} and zinc proteins.³⁴

For randomly oriented molecules, the EXAFS technique provides radial distance information only; structural arrangement of atoms must be deduced. Resonance Raman spectroscopy measures molecular vibration modes of metal-ligand bonds in metalloproteins coupled to resonantly laser-

excited electronic transitions.³⁵ The frequencies and intensities of these modes are sensitive to geometry as well as to ligand type. Consequently, EXAFS and resonance Raman spectroscopy are capable of providing complementary and mutually supportive information, as demonstrated here for Hc.

Experimental Section

Hc from a mollusc, *Busycon canaliculatum*, was chosen for investigation because of its ease of preparation and because mollusc Hc has a higher copper concentration (0.25–0.26%) than arthropod Hc (0.17–0.18%).^{3–5} Also, the UV resonance Raman spectrum is better resolved for mollusc than for arthropod Hc.^{1,36} *Busycon canaliculatum* specimens were obtained from Marine Biological Laboratories, Woods Hole, Mass. The shells were fractured to expose the cardiac chamber, and the hemolymph was drained by heart puncture. Protein samples were centrifuged at low speed to remove shell fragments and other debris, and were exhaustively dialyzed against distilled water. Zinc, which interferes with the EXAFS measurements, was removed from the samples either by dialysis against several changes of 25 mM EDTA and then against distilled water, or by passage through a 10 × 100 mm Chelex 100 ion exchange column. The Hc was pelleted by centrifuging for 4–6 h at 45000g to separate out lower molecular weight protein contaminants. Hc concentrations were determined from the absorbance at 345 nm ($\epsilon = 10\,000\text{ M}_{\text{Cu}}^{-1}\text{ cm}^{-1}$). EXAFS measurements were carried out on lyophilized samples prepared with a quantity of sucrose equal to the weight of the protein, to prevent denaturation. For oxyHc, the powder was exposed to air after removal from the vacuum to ensure complete oxygenation. For deoxyHc, the protein sucrose solution was deoxygenated by equilibration with water-saturated argon, lyophilized, stored under argon, and maintained at liquid nitrogen temperatures to prevent oxygenation. Authentic oxyHc optical spectra were obtained upon dissolving the irradiated powders in oxygenated water. Concentrated solution samples were employed for edge studies, deoxyHc being obtained by dithionite addition.

Model Complexes. Several copper complexes were used to model and calibrate various aspects of the X-ray data—(1) aqueous copper(II) imidazole: 10^{-3} mol of $\text{CuSO}_4 \cdot 5\text{H}_2\text{O}$ was dissolved in 10 mL of a 5 M solution of imidazole in distilled water; (2) aqueous copper(I) imidazole: the solution from the above preparation was reduced by the addition of excess sodium dithionite; (3) $\text{Cu}^{\text{II}}[\text{Im}]_4 \cdot \text{SO}_4$ (CuIm):³⁷ 40 mL of 1 M imidazole and 10 mL of 1 M $\text{CuSO}_4 \cdot 5\text{H}_2\text{O}$ were mixed, and the deep blue crystals were obtained by slow evaporation; (4) $\text{Cu}^{\text{II}}[\text{Im}]_3 \cdot \text{H}_2\text{O} \cdot \text{SO}_4$:³⁸ 30 mL of 1 M imidazole and 10 mL of 1 M $\text{CuSO}_4 \cdot 5\text{H}_2\text{O}$ were mixed, and the pH was adjusted to 6.5 by the addition of 0.1 N H_2SO_4 ; deep blue crystals were obtained by slow evaporation; (5) aqueous copper(I) cyanide: 2×10^{-3} mol of $\text{CuSO}_4 \cdot 5\text{H}_2\text{O}$ and 0.1 mol of KCN were dissolved in 10 mL of distilled water; (6) copper(I) *n*-butylmercaptide: 10^{-3} mol of $\text{CuSO}_4 \cdot 5\text{H}_2\text{O}$ and 0.02 mol of sodium *n*-butylthiolate were dissolved in 10 mL of distilled water; (7) copper(II) tetraphenylporphine (CuTPP) was prepared as described in the literature;³⁹ (8) $\text{Cu}^{\text{II}}(\text{gly})_2 \cdot \text{H}_2\text{O}$: bis-(glycinato)copper(II) monohydrate was prepared as described in the literature;⁴⁰ (9) $[\text{bpyCu}^{\text{II}}\text{OH}]_2 \cdot \text{SO}_4 \cdot 5\text{H}_2\text{O}$ (CuBpy):⁴¹ 50 mL of 0.1 M NaOH was added to a suspension of 1.43 g of $\text{CuSO}_4 \cdot 5\text{H}_2\text{O}$ and 0.89 g of 2,2'-bipyridyl in 20 mL of water; the solution was heated to boiling, then cooled to 4 °C to precipitate the complex, which was recrystallized from water and washed with dry ether; (10) $[\text{tmen-Cu}^{\text{II}}\text{OH}]_2 \cdot \text{Br}_2$ ⁴² (Cutmen): tmen (*N,N,N,N*-tetramethylethylenediamine) was added (~20 mL total) dropwise to a solution of 10 g of CuBr_2 and 80 mL of H_2O until the initial green precipitate redissolved; the solution was concentrated over a steam bath and allowed to evaporate and dry in air; dark burgundy colored crystals were obtained; (11) $[\text{2-picCu}^{\text{II}}]_2 \cdot \text{Br}_2$:⁴³ excess 2-pic (2-methylpyridine) was added to a solution of CuBr_2 , and the solution was heated to near boiling; the crystals obtained upon cooling were recrystallized from absolute methanol; (12) $\text{Cu}^{\text{II}}[\text{CH}_3\text{COO}]_2 \cdot \text{H}_2\text{O}$ (CuAc): copper(II) acetate monohydrate was obtained from Fisher Scientific Co. and used without further publication.

X-ray measurements were conducted at the Stanford Synchrotron Radiation Laboratory, during June and November 1976 and December 1977, at SPEAR energies in excess of 3 GeV. The model complexes and copper metal were measured in transmission using the EXAFS I beam line,⁴⁴ while protein data was obtained with a nine-element array of scintillation counters to monitor the Cu $K\alpha$ fluo-

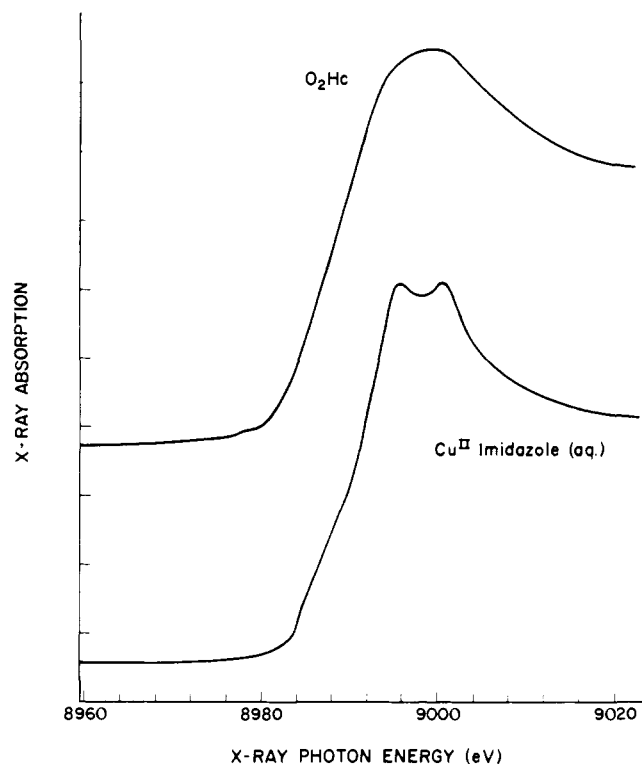


Figure 1. Copper K edge absorption spectra of oxyHc and aqueous copper(II) imidazole.

rescence. The samples were mounted in Plexiglass sample holder windows, sufficiently large to avoid interference with the X-ray beam, and contained by Kapton or Mylar film. Low-temperature data for deoxyhemocyanin and copper metal were obtained at 77 K.

Prior to analysis, the experimental data were converted from the monochromator angle (Bragg angle) scale to an X-ray photon energy scale, standardized to the sharp 4p peak (8996 eV) in the absorption edge of $\text{CuCl}_2 \cdot 2\text{H}_2\text{O}$. The reported energy values are accurate to within the ± 0.5 eV resolution of the crystal monochromator.

Results

Absorption Edges. Figure 1 shows the X-ray absorption spectrum in the region of the Cu K edge for oxyhemocyanin and aqueous copper(II) imidazole, while Figure 2 shows spectra for deoxyhemocyanin and aqueous copper(I) imidazole. The absorption edge maximum in each case corresponds to the allowed $1s \rightarrow np$ ($n \geq 4$) transitions which merge into the continuum at higher energy. Below the maximum are subsidiary peaks and shoulders reflecting transitions to empty orbitals,^{45a} e.g., $1s \rightarrow 3d$ and $1s \rightarrow 4s$. Their intensities are expected to be governed by dipole selection rules, $1s \rightarrow 3d$ and $1s \rightarrow 4s$ being weaker than $1s \rightarrow 4p$. Strong $1s \rightarrow 4p$ and weaker $1s \rightarrow 4s$ transitions can be discerned at 8992 and 8982 eV for Cu(I) compounds (Figure 2) and at 8992–9002 and 8987 eV for Cu(II) complexes (Figure 1). The similarity in the Cu(II) and Cu(I) energies is consistent with detailed edge studies by Blumberg et al.,^{46b} which show considerable overlap in the observed energy ranges for these transitions in complexes which are formally Cu(I) and Cu(II).

A comparison of the relative transition intensities can yield useful chemical information. In the first place, only Cu(II) can give rise to a $1s \rightarrow 3d$ transition, the 3d levels being filled in Cu(I).

A very weak feature at 8978 eV is observable for Cu(II) complexes, being absent in the Cu(I) complexes (Table I), and is reasonably assigned to the $1s \rightarrow 3d$ transition. This feature can be observed in the oxyhemocyanin spectrum and confirms the Cu(II) oxidation state in this protein. The $1s \rightarrow 4s$ transition is seen distinctly for $\text{Cu}^{\text{II}}\text{TPP}$ and for copper(II) acetate,

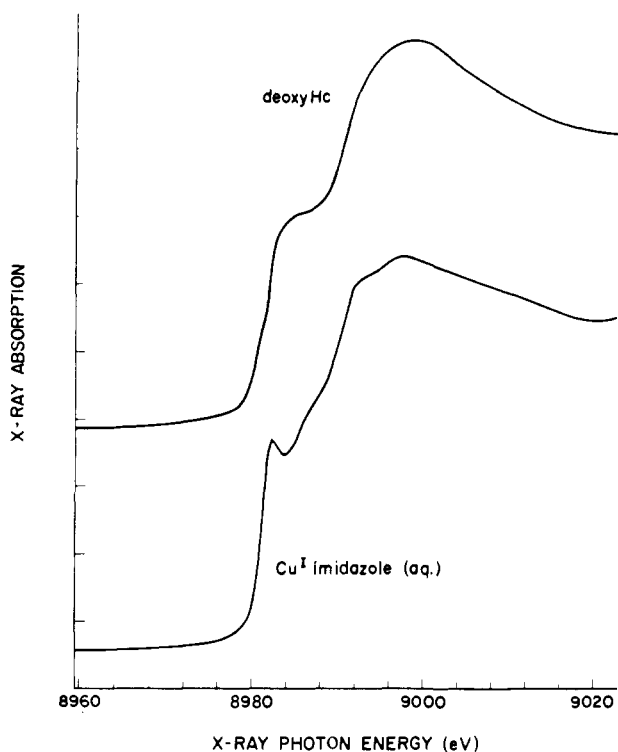


Figure 2. Copper K edge absorption spectra of deoxyHc and aqueous copper(I) imidazole.

but is indistinct for aqueous copper(II) imidazole, and is likewise unresolved for oxyhemocyanin. For the Cu(I) complexes, the $1s \rightarrow 4s$ transition (the first peak in the spectra of Figure 2) is more intense than it is for the Cu(II) complexes, consistent with the proclivity of Cu(I) for geometries, e.g., trigonal or distorted tetrahedral, which allow s - p mixing. Copper(I) imidazole shows a $1s \rightarrow 4s$ peak which is about half the height of the $1s \rightarrow 4p$ maximum, as does deoxyhemocyanin. Dithionite reduction demonstrates that this shoulder height is characteristic of a totally reduced species in both the model and protein. Subsequent exposure to air decreases the shoulder height in both samples until the Cu(II) edge spectra (Figure 1) are again obtained. The close similarity of the edge structure of oxy- and deoxyhemocyanin with Cu(II) and Cu(I) imidazole, respectively, is consistent with imidazole coordination in both forms of the protein.

In the Cu(II) complex spectra, multiple peaks and shoulders are observed in the high absorption region corresponding to $1s \rightarrow 4p$ transitions, consistent with coordination geometry inequivalencies of p_x , p_y , and p_z . Strong anisotropy is expected for the tetragonal coordination geometry typical of Cu(II) ($p_x = p_y > p_z$ in energy). Less structure is seen in the $1s \rightarrow 4p$ region of the Cu(I) complex spectra, consistent with more isotropic character. For oxyhemocyanin the $1s \rightarrow 4p$ absorption is broad but unstructured, suggesting a somewhat irregular coordination geometry.

EXAFS Analysis. The CuTPP, copper metal, other Cu-N and Cu-Cu model compounds, and signal averaged protein X-ray absorption data were converted to EXAFS modulation spectra employing a cubic spline fit background subtraction.^{30a} Although the zinc contamination of the protein samples was considerably reduced in magnitude by the procedures described in the Experimental Section, a zinc edge was still apparent in the spectra. Consequently, the protein data were truncated directly below the zinc edge, at $k = 13.5 \text{ \AA}^{-1}$, prior to background subtraction. In practice, the EXAFS signal was negligible beyond the cutoff. Figure 3 shows the Fourier transforms of the EXAFS.^{30a,b}

Table I. K Edge Peak Positions and Approximate Widths at Half-Height for Hemocyanins and Copper Model Complexes^a

complex				
aq Cu(II) imidazole			—Δ—Δ—	
Cu ^{II} TPP	—○—	—x—	—Δ—Δ—	
Cu ^{II} (gly) ₂ ·H ₂ O	—○—	—x—	—Δ—Δ—	
Cu ^{II} (CH ₃ COO) ₂ ·H ₂ O	—○—	—x—	—Δ—Δ—	
oxyhemocyanin	—○—		—Δ—Δ—	
aq Cu(I) imidazole		—x—	—Δ—Δ—	
aq Cu(I) <i>n</i> -butylmercaptide		—x—	—Δ—Δ—	
aq Cu(I) cyanide		—x—	—Δ—Δ—	
deoxyhemocyanin		—x—	—Δ—Δ—	
X-ray photon energy, eV				
			8970	8980
			8990	9000
			9010	

^a O, $1s \rightarrow 3d$; X, $1s \rightarrow 4s$; Δ, $1s \rightarrow 4p$.

Table II. Protein Parameters from First-Shell Fourier-Filtered EXAFS Data

parameter ^a	CuTPP reference for protein			
	oxyHc		deoxyHc	
$R (\text{Å}) \pm 0.03$	1.96	1.96	1.95	1.95
$N \pm 1.5$	3.5	3.2	2.0	1.4
$\Delta\sigma^2$	0	7.3×10^{-4}	0	-3.0×10^{-3}

^a Symbols: R , average distance; N , number of scattering atoms; $\Delta\sigma^2$, change in mean square displacement (Debye-Waller factor) relative to the reference. In each case, the change in edge energy relative to the reference was small ($< \sim 1$ eV).

First Coordination Shell. The most prominent peak in the Fourier transform arises from nearest neighbor scattering. This peak, when isolated using Fourier filtering, and transformed back to k space, closely resembles the first shell (Cu-N) EXAFS for CuTPP and CuIm. Since the number of nearest neighbor atoms (four) and their distances⁴⁶ are known for these two model compounds, the Fourier-filtered model data were used as references for the protein data, employing the concept of chemical transferability of phase.⁴⁷ The filtering technique is described in detail elsewhere.³⁰

In this work we used a curve-fitting technique to analyze the filtered data. First, empirical amplitude and phase information was extracted from the model compound data.^{30a} We then tried to fit filtered protein data with the empirical data, allowing the overall amplitude N , threshold energy E_0 , distance R , and Debye-Waller σ^2 to vary. Thus, at most four adjustable parameters were used in a fit. By comparing experimental data with model data in this way, only the ratio of amplitudes (N_1/N_2), the change in threshold energy (ΔE_0), the change in R (ΔR), and the change in σ^2 ($\Delta\sigma^2$) are significant. The parameter $\Delta\sigma^2$ is *positive* if the model compound data had to be *amplified* for large k values to fit the protein data. Since σ^2 contains information about both static structural disorder and thermal vibrations,^{31b} a positive $\Delta\sigma^2$ as a fitting result is an indication that something is wrong, since in the models we used, both the static disorder and the thermal vibrations were small, as estimated from X-ray diffraction results and vibrational spectrum information, with the net value of σ being about 0.05 \AA .

For each fit an eigenvalue-eigenvector analysis was done to discover any parameter correlation effects and to get an estimate of the sensitivity of the fit to the various parameters and hence error estimates for the parameters.^{30c,d} In this way we determined that the change in distance ΔR is essentially

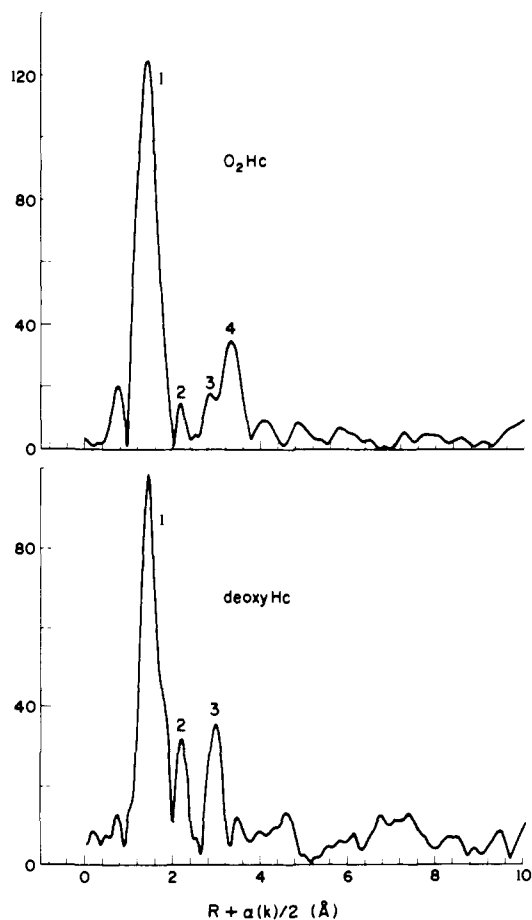


Figure 3. Fourier transforms of EXAFS data for oxy- and deoxyHc.

uncorrelated with the amplitude determining parameters N_1/N_2 and $\Delta\sigma^2$, and only slightly dependent on ΔE_0 . Also, the amplitude ratio and the change in σ^2 were somewhat correlated, thus increasing the error bars on N_1/N_2 .

Table II lists the resulting parameters. Model compounds for Cu–N distances showed no changes in distance and little change in Debye–Waller factor between room and liquid nitrogen temperatures. A satisfactory fit was obtained using a fixed Debye–Waller factor correction of zero when comparing CuTPP and the proteins; the fit was improved somewhat by allowing the Debye–Waller factor to vary. This variation had a negligible effect on the average distances, 1.96 Å for oxyHc and 1.95 Å for deoxyHc. It had a substantial effect on the estimated number of nearest neighbors, N , since both σ^2 and N directly affect the amplitude of the EXAFS modulation. The number of backscattering atoms is much less certain than the average distance. The calculated numbers do indicate, however, that there is a substantial increase in the Cu coordination number between deoxy- and oxyHc.

Copper–Copper Distances. The Hc Fourier spectra also show distinct outer shell peaks, marked 4 for oxyHc and 3 for deoxyHc in Figure 3, which are logical candidates for the expected Cu–Cu interaction. (The additional, weaker features cannot confidently be distinguished from noise or truncation errors.)

In order to compare model compounds with these outer protein shells, the outer shells of the model compounds must be examined for mean free path effects and comparison of $\Delta\sigma^2$ with the first shell. In both CuTPP and Cu metal, successive outer shells could be satisfactorily fit to the first shell with $\Delta\sigma^2 = 0$ and average distances and numbers of scattering atoms the same within fitting error as those obtained from X-ray crystallography. Accordingly, the outer shell data were ref-

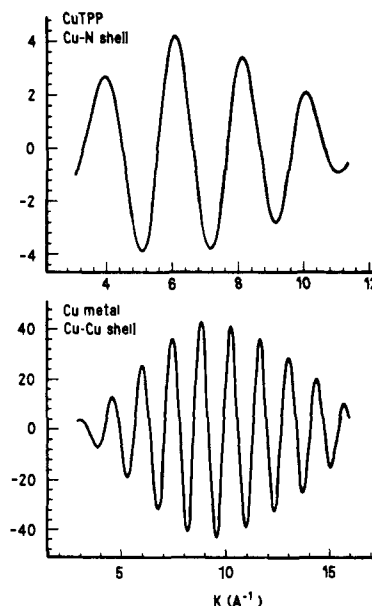


Figure 4. Back-transformed filtered EXAFS data for first shells of CuTPP (Cu–N) and of Cu metal (Cu–Cu).

Table III. Protein Parameters from Outer-Shell Fourier-Filtered EXAFS Data

parameter ^a	protein			
	oxyHc		deoxyHc	
	Cu metal (77 K) ref		Cu metal (77 K) ref	CuTPP ref
R (Å) ± 0.05	3.68	3.68	3.39	3.44
$N \pm 0.2$	1.4	1.0	0.99	1.7
$\Delta\sigma^2$	0	-3.4×10^{-3}	-7.3×10^{-3}	2.4×10^{-3}

^a Symbols are as in Table II. In each case, the change in edge energy relative to the reference was small ($< \sim 1$ eV).

erenced to the first shell spectrum of Cu metal, with the results shown in Table III. For oxyHc a satisfactory fit was obtained, which improved on allowing $\Delta\sigma^2$ to vary. As with the first shell, this variation had a negligible effect on the distance, 3.67 Å, but an appreciable effect on N , which decreased to the expected value of 1.0. For deoxyHc a satisfactory fit could only be obtained with a decrease in $\Delta\sigma^2$, relative to Cu metal; the expected N value, 1.0, was obtained.

The question arises whether the outer shell peak could result from backscattering by atoms in the protein other than Cu. This was examined by plotting the amplitude function of the filtered EXAFS data, since it is expected⁴⁸ to maximize at higher k for heavy atoms than for light atoms. As shown in Figure 4, the amplitudes maximize at ~ 5 and ~ 10 Å, respectively, for the first shell data of CuTPP (Cu–N) and Cu metal (Cu–Cu). Figure 5 gives the outer shell back-transformed data for the proteins. For oxyHc, the outer shell amplitude maximizes at $k \approx 9$ Å, confirming a dominant Cu–Cu contribution. For deoxyHc, however, the amplitude function is broad, with a maximum near 7 Å.

Consistent with this difference, the oxyHc outer shell data could not be fit with a Cu–N structure with CuTPP as reference, but it was possible to fit deoxyHc in this way, with the parameters shown in Table III. Both N and $\Delta\sigma^2$ are satisfactory. The distance, 3.44 Å, is essentially the same as that estimated for a Cu–Cu structure. It is about 75% larger than a normal Cu–N bond distance (approximately 2.0 Å). Conceivable candidates for the interaction are the ring atoms of imidazole groups involved in Cu ligation.^{37,38} As illustrated

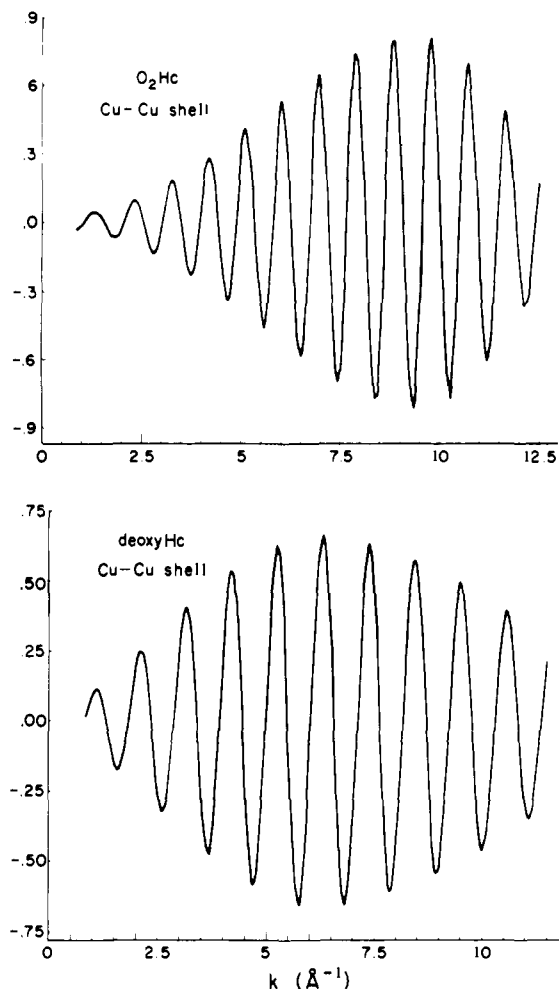


Figure 5. Back-transformed filtered EXAFS data for oxy- and deoxyHc.

in Figure 6, however, 3.44 Å lies half-way between the second and third shell distances expected for coordinated imidazole. The third shell distances might be decreased somewhat by tilting of the imidazole ring, but the degree of tilt required to reduce them to 3.44 Å is excessive. In order to investigate this situation further, several model compounds having different distances and kinds of bridges between Cu atoms were investigated. These copper outer shells were then fitted by Cu-N amplitude and phase, using CuTPP as a model, and the resulting parameters are given in Table IV. In each case a positive $\Delta\sigma^2$ is required for a satisfactory fit, and the average distance (R) is slightly larger (although generally within the error). In Cutmen and Cubpy the number of scatters (N) is also too large. On the other hand, using Cu metal as a model produces agreement with crystallographic data with reasonable $\Delta\sigma^2$ values. These trends of large N , R , and positive $\Delta\sigma^2$ are observed for the deoxyHc outer shell fit to a Cu-N reference (Table III), while the Cu metal fit is very similar to that of the model compounds.

These considerations make a Cu-Cu assignment of the outer shell deoxyHc peak much likelier than a Cu first-row atom assignment, but the distinction cannot be made by EXAFS criteria alone, at the present level of data quality.

Discussion

The present EXAFS analysis allows the following inferences about the hemocyanine binding site:

1. The Cu-Cu distance in oxyHc is 3.67 Å, which is short enough to allow O₂ to bind as a bridging ligand. This distance appears to decrease slightly, to 3.39 Å, upon deoxygenation.

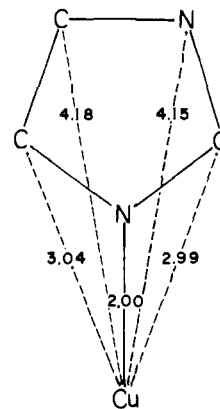


Figure 6. Cu-N and Cu-C distances for coordinated imidazole; average of seven observed distances in Cu^{II}Im₄SO₄ and Cu^{II}Im₃·H₂O·SO₄.

Table IV. Model Compound Parameters

compd	parameter ^a	CuTPP ref	Cu metal (300 K) ref
CuTPP	R (Å) ± 0.03	1.98	2.00
1st shell ^b	N ± 0.5	4.0	2.7
(1.984, 4) ³⁸	$\Delta\sigma^2$	-1.2×10^{-5}	-7.4×10^{-3}
CuIm	R (Å) ± 0.03	2.01	2.00
1st shell ^b	N ± 0.5	3.3	5.3
(2.01, 4) ³⁷	$\Delta\sigma^2$	-3.1×10^{-3}	-1.1×10^{-2}
Cu metal (300 K)	R (Å) ± 0.03	2.53	2.55
1st shell ^b	N ± 1.8	8.35	12.0
(2.55, 12) ⁵⁶	$\Delta\sigma^2$	7.4×10^{-3}	-7.0×10^{-6}
Cu metal (77 K)	R (Å) ± 0.03		2.55
1st shell ^b	N ± 1.8		13.7
(2.55, 12) ⁵⁶	$\Delta\sigma^2$		6.8×10^{-3}
Cutmen	R (Å) ± 0.04	3.06	3.03
outer shell	N ± 0.3	1.4	1.0
(3.00, 1) ⁴²	$\Delta\sigma^2$	7.0×10^{-3}	-2.0×10^{-4}
Cubpy	R (Å) ± 0.04	2.97	2.93
outer shell	N ± 0.3	1.87	1.2
(2.89, 1) ⁴¹	$\Delta\sigma^2$	1.0×10^{-2}	8×10^{-4}
CuAc	R (Å) ± 0.04	2.67	2.63
outer shell	N ± 0.4	0.46	0.48
(2.64, 1) ⁵⁷	$\Delta\sigma^2$	9.2×10^{-3}	2.8×10^{-3}

^a Symbols are as in Table II. In each case the change in edge energy relative to the reference was small (<4 eV). ^b Distance (Å) and number of atoms are given in parentheses; successive outer shells of CuTPP and Cu metal could be satisfactorily fit with the first shell for $\Delta\sigma^2 = 0$ (see text).

This result would imply that there is no large-scale conformation change of the active site upon oxygen binding. A less likely interpretation of the deoxyHc data is that the 3.4-Å interaction is due to some atom other than Cu.

2. The edge structures are consistent with Cu(II) and Cu(I) bound to imidazole in oxy- and deoxyHc, respectively.

3. The average nearest neighbor distance is essentially the same, 1.96 and 1.95 Å in oxy- and deoxyHc, respectively. The number of nearest neighbors, however, decreases substantially. First-shell data fitting gives $N = 3.2$ -3.4 for oxyHc and 1.4-2.0 for deoxyHc, although large uncertainties are associated with these estimates.

The apparent 30-50% decrease in coordination number between oxy- and deoxyHc suggests that two ligand atoms are lost upon deoxygenation. Loss of the dioxygen molecule itself might account for the decrease, if both oxygen atoms are equidistant from each of the Cu atoms in oxyHc. (EXAFS is monitored for both copper atoms, and the intensity measurements are on a per copper basis.) This would require that the dioxygen molecule lie across the copper-copper vector at an

angle of 90° . Sideways binding of dioxygen to metal ions is well known, and is in fact characteristic of peroxide bound to mononuclear transition metal complexes.⁴⁹ It has not been observed, however, in binuclear complexes, for which the O–O bond is generally found at a fairly acute angle to the metal–metal axis, as in $[(\text{NH}_3)_5\text{Co}^{\text{III}}(\text{O}_2)\text{Co}^{\text{III}}(\text{NH}_3)_5]^{4+}$.⁵⁰ On the other hand, most known binuclear peroxo adducts are cobalt complexes, and may not be apt models for the binuclear copper site in hemocyanin. The Co–Co distance in the pentaammine complex⁵⁰ is 4.5 Å, 0.8 Å longer than the Cu–Cu distance in oxyHc. The requirement for 90° orientation is quite stringent if both oxygen atoms are to contribute to the first-shell peak. We calculate that a deviation of over 5° would produce over a 0.1-Å difference in the distances of the two oxygen atoms from either copper atom, which should begin to produce appreciable broadening of the first peak. A deviation of over 10° would increase the difference to above 0.2 Å, sufficient to remove one of the oxygen atoms altogether from the peak.

An alternative interpretation is that only one of the O_2 atoms contributes to the first shell peak, and that an additional ligand atom is lost upon deoxygenation. This might be an atom that bridges the Cu(II) ions in oxyHc, but that does not bind to the Cu(I) ions of deoxyHc. A bridging ligand in addition to O_2 is suggested^{7,51} by the fact that it is possible to prepare an oxidized form of Hc, metHc,^{3–57} that contains no dioxygen, yet in which the Cu(II) ions are still antiferromagnetically coupled. Since this coupling implies the presence of a non- O_2 bridge in metHc, it is plausible, although by no means required, that the same bridge be present in oxyHc, which can in some cases be prepared from metHc by addition of peroxide.⁵¹ A prime candidate for the extra bridging ligand is tyrosine,⁷ since an absorption shoulder in low-temperature spectra is observable for both oxy- and metHc at ~ 400 nm, a reasonable energy for a phenolate to copper charge-transfer transition. Dissociation of the bridging tyrosine upon deoxygenation would make sense chemically since the “soft” Cu(I) ion is not avid for oxygen ligands. On the other hand, the bridging atom need not move far away (≥ 0.2 Å) to be lost from the first-shell peak.

If the loss of two ligand atoms per Cu between oxy- and deoxyHc is accepted, then plausible coordination numbers are six and four, five and three, or four and two for oxy- and deoxyHc, respectively. Six-coordinate Cu(II) is well known, but the complexes are always tetragonal with two axial bonds that are substantially longer (>0.2 Å) than the four equatorial bonds. It is unlikely that two axial atoms could contribute appreciably to the first-shell EXAFS Fourier peak. Preliminary experiments indicate that tetragonal Cu(II) complexes give first-shell intensities corresponding to four coordination. Five-coordinate Cu(II) is also well known, both trigonal- and square-based pyramidal geometries being common. Although the spread in distances between axial and equatorial or basal bonds is often substantial, there is precedent for Cu(II) with five distances within a range of 0.08 Å.⁵² If this were the situation in oxyHc, all five ligand atoms would be expected to contribute to the first-shell EXAFS Fourier peak. For Cu(I), four, three, and two are all well-established coordination numbers.⁵³

The EXAFS nearest neighbor numbers are most consistent with four-coordinate Cu(II) and two-coordinate Cu(I), but they may well be in error by one or more units. The UV resonance Raman spectrum of oxyHc is most straightforwardly interpreted in terms of three imidazole ligands;¹ this number also accords with the imidazole photooxidation stoichiometry.^{16,17} Consequently, we think it likely that the coordination number is five for oxyHc (three imidazoles, O_2 , and the putative extra bridging ligand) and three for deoxyHc, the three imidazoles presumably remaining bound to Cu(I). The oxyHc resonance Raman spectra suggest that one of the copper–imidazole bonds has a lowered stretching frequency, and

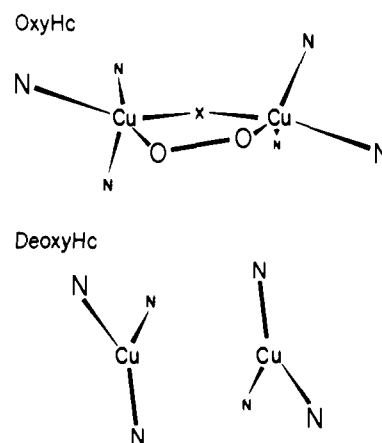


Figure 7. Suggested model for the Hc binding site.

presumably a slightly larger bond distance, than the other two.

These considerations lead us to construct a model of the oxyHc active site, as shown in Figure 7. This model is similar to that which has been emerging from the various physicochemical studies of hemocyanin (cf, e.g., Amundsen et al.¹⁷) but is more specific in structural detail. Several of its features are suggested by the recent work of Solomon and co-workers.^{7,51,54,55} Each Cu(II) ion is drawn as having a square-pyramidal coordination group, the basal plane being defined by the bridging dioxygen and tyrosine oxygen atoms and two of the imidazole ligands,⁵⁴ the third imidazole forming the slightly weaker axial bond. The angle of the oxygen–oxygen bond with respect to the copper–copper axis cannot be determined from the available data. It could be as small as 0° or as large as 80° . It could also be 90° , but in that case we would remove the bridging tyrosine from the model and rearrange the basal plane to contain both the oxygen atoms of the dioxygen molecule. Upon deoxygenation, the bridging tyrosine is suggested to be removed to a nonbonding distance, leaving Cu(I) bound to the three imidazoles, presumably in a trigonal-planar arrangement.⁵² The copper atoms are slightly closer than in oxyHc, but the 3.4-Å separation is an adequate nonbonded distance and poses no particular steric problem. There must, however, be a fairly special protein architecture to prepare the two Cu(I) centers in just this manner.

The symmetry of the Hc site need not be as high as indicated in Figure 7. Although a square-based pyramid has been chosen for the Cu(II) coordination group because of the evidence from electronic spectroscopy that the Cu(II) ions are basically tetragonal,^{7,54} appreciable angular deviations from the basal plane could, no doubt, occur. The ^{16}O – ^{18}O resonance Raman study by Loehr and co-workers⁵⁶ established that the two ends of the bound dioxygen molecule are equivalent, in contrast to the situation found in hemerythrin,⁵⁷ so that the two Cu(II) ions cannot be too dissimilar electronically. Nevertheless, appreciable geometric differences between the two copper coordination groups could probably be tolerated and are not inconsistent with the UV resonance Raman spectra.¹

Acknowledgment. We thank Drs. P. Eisenberger and E. I. Solomon for helpful discussions, and Dr. J. A. Kincaid for providing the copper TPP and copper glycinate samples. This work was supported by National Institutes of Health Grant GM13498 to T.G.S.

References and Notes

- (1) Part 2: J. A. Larrabee and T. G. Spiro, *J. Am. Chem. Soc.*, following paper in this issue.
- (2) (a) Princeton University. (b) Exxon Research & Engineering Co., Linden, N.J. 07036. (c) Bell Telephone Laboratories.

- (3) F. Ghirelli, Ed., "Physiology and Biochemistry of Hemocyanins", Academic Press, New York, 1968.
- (4) K. E. Van Holde and E. F. J. Van Bruggen in "Subunits in Biological Systems", Part A, S. N. Timasheff and E. D. Fasman, Eds., Marcel Dekker, New York, 1971, pp 1-53.
- (5) R. Lontie and L. Vanquickenborne in "Metal Ions in Biological Systems", Vol. 3, H. Siegel, Ed., Marcel Dekker, New York, 1974, pp 183-200.
- (6) K. W. Nickerson and K. E. Van Holde, *Comp. Biochem. Physiol.*, **39B**, 855 (1971).
- (7) R. S. Himmelwright, N. C. Eickman, and E. I. Solomon, *Proc. Natl. Acad. Sci. U.S.A.*, **78**, 2094 (1979).
- (8) J. S. Loehr, T. B. Freedman, and T. M. Loehr, *Biochem. Biophys. Res. Commun.*, **56**, 510 (1974).
- (9) T. B. Freedman, J. S. Loehr, and T. M. Loehr, *J. Am. Chem. Soc.*, **98**, 2809 (1976).
- (10) E. Frieden, S. Osaki, and H. Kobayashi, *J. Gen. Physiol.*, **49**, 213 (1965).
- (11) T. H. Moss, D. C. Gould, A. Ehrenberg, J. S. Loehr, and H. S. Mason, *Biochemistry*, **12**, 1244 (1973).
- (12) E. I. Solomon, D. M. Dooley, R. H. Wang, H. B. Gray, M. Cerdonio, F. Mogno, and G. L. Romani, *J. Am. Chem. Soc.*, **98**, 1029 (1976).
- (13) A. J. M. School Uiterkamp, H. Vander Deen, H. C. J. Berendsen, and J. F. Beos, *Biochim. Biophys. Acta*, **372**, 407 (1974).
- (14) B. Salvato, A. Ghirelli-Magaldi, and F. Ghirelli, *Biochemistry*, **13**, 4778 (1974).
- (15) Y. Engelborgh and R. Lontie, *Eur. J. Biochem.*, **39**, 335 (1973).
- (16) L. Tallandi, B. Salvato, and G. Jori, *FEBS Lett.*, **64**, 283 (1975).
- (17) A. R. Amundsen, J. Wheland, and B. Bosnich, *J. Am. Chem. Soc.*, **99**, 6730 (1977).
- (18) E. J. Wood and W. H. Banister, *Biochim. Biophys. Acta*, **154**, 10 (1968).
- (19) N. Shaklai and E. Daniel, *Biochemistry*, **9**, 564 (1970).
- (20) R. Lontie, *Clin. Chim. Acta*, **3**, 68 (1958).
- (21) J. A. Wurzbach, P. J. Grunther, D. M. Dooley, H. B. Gray, and E. I. Solomon, *J. Am. Chem. Soc.*, **99**, 1257 (1977).
- (22) N. Makino, P. McMakill, and H. S. Mason, *J. Biol. Chem.*, **249**, 6062 (1974).
- (23) R. L. Jolley, L. H. Evans, N. Makino, and H. S. Mason, *J. Biol. Chem.*, **249**, 335 (1974).
- (24) K. Lerch, *FEBS Lett.*, **69**, 157 (1976).
- (25) N. Eickman, J. A. Larrabee, E. I. Solomon, C. Lerch, and T. G. Spiro, *J. Am. Chem. Soc.*, **100**, 6529 (1978).
- (26) J. Fee, *Struct. Bonding (Berlin)*, **23**, 1-60 (1975).
- (27) K. E. Falk, T. Vannard, and J. Angstrom, *FEBS Lett.*, **75**, 23 (1977).
- (28) H. A. Kuiper, W. Gaastra, J. J. Beintema, E. F. J. Van Bruggen, A. M. H. Schefman, and J. Drenth, *J. Mol. Biol.*, **99**, 619 (1975).
- (29) (a) K. A. Magnus and W. E. Love, *J. Mol. Biol.*, **116**, 171 (1977). (b) W. E. Love, personal communication.
- (30) (a) P. Eisenberger and B. M. Kincaid, *Science*, **200**, 1441 (1978). (b) D. E. Sayers, F. W. Lyle, and E. A. Stern, *Adv. X-Ray Anal.*, **13**, 248 (1970). (c) C. Lanczos, "Applied Analysis", Prentice-Hall, Englewood Cliffs, N.J., 1956. (d) C. L. Lawson and R. J. Hanson, "Solving Least-Squares Problems", Prentice-Hall, Englewood Cliffs, N.J., 1974.
- (31) (a) R. G. Shulman, P. Eisenberger, W. E. Blumberg, and N. A. Stombaugh, *Proc. Natl. Acad. Sci. U.S.A.*, **72**, 4003 (1975). (b) R. G. Shulman, P. Eisenberger, B. K. Teo, B. M. Kincaid, and G. S. Brown, *J. Mol. Biol.*, **124**, 305 (1978).
- (32) (a) P. Eisenberger, R. G. Shulman, G. S. Brown, and S. Ogawa, *Proc. Natl. Acad. Sci. U.S.A.*, **73**, 491 (1976). (b) P. Eisenberger, R. G. Shulman, G. S. Brown, and S. Ogawa, *Nature (London)*, **274**, 30 (1970).
- (33) (a) S. P. Cramer, K. O. Hodgson, W. O. Gillum, and L. E. Mortensen, *J. Am. Chem. Soc.*, **100**, 3398 (1978). (b) S. P. Cramer, H. B. Gray, and K. V. Rajagopalan, *ibid.*, **101**, 2770 (1979). (c) T. D. Tullius, D. M. Kurtz, Jr., S. D. Conradson, and K. O. Hodgson, *ibid.*, **101**, 2776 (1979). (d) T. D. Tullius, P. Frank, and K. O. Hodgson, *Proc. Natl. Acad. Sci. U.S.A.*, **75**, 4069 (1978).
- (34) G. S. Brown, G. Navon, and R. G. Shulman, *Proc. Natl. Acad. Sci. U.S.A.*, **74**, 1794 (1977).
- (35) (a) T. G. Spiro and P. Stein, *Annu. Rev. Phys. Chem.*, **28**, 501 (1977). (b) T. G. Spiro and T. M. Loehr, *Adv. Infrared Raman Spectrosc.*, **1**, 98 (1975). (c) T. G. Spiro and B. P. Gaber, *Annu. Rev. Biochem.*, **46**, 553 (1977).
- (36) J. A. Larrabee, T. G. Spiro, N. S. Ferris, W. H. Woodruff, W. A. Maltese, and M. S. Kerr, *J. Am. Chem. Soc.*, **99**, 1979 (1977).
- (37) G. Fransson and B. K. S. Lundberg, *Acta Chem. Scand.*, **26**, 3969 (1972).
- (38) G. Fransson and B. K. S. Lundberg, *Acta Chem. Scand., Ser. A.*, **28**, 578 (1974).
- (39) K. M. Smith, "Porphyrins and Metalloporphyrins", Elsevier, New York, 1975.
- (40) J. R. Kincaid and K. Nakamoto, *Spectrochim. Acta, Ser. A*, **32**, 277 (1976).
- (41) (a) C. M. Harris, E. Sinn, W. R. Walker, and P. R. Wooliams, *Aust. J. Chem.*, **21**, 631 (1968). (b) A. T. Casey, B. F. Hoskins, and F. D. Whillans, *Chem. Commun.*, 904 (1974).
- (42) (a) J. R. Wasson, T. P. Mitchell, and W. H. Bernard, *J. Inorg. Nucl. Chem.*, **30**, 2865 (1968). (b) T. P. Mitchell, W. H. Bernard, and J. R. Wasson, *Acta Crystallogr., Sect. B*, **26**, 2096 (1970).
- (43) P. Singh, D. Y. Jeter, W. E. Hatfield, and D. J. Hodgson, *Inorg. Chem.*, **11**, 1657 (1972).
- (44) B. M. Kincaid, Ph.D. Thesis, Stanford University, Stanford, Calif., 1975.
- (45) (a) R. G. Shulman, Y. Yafet, P. Eisenberger, and W. E. Blumberg, *Proc. Natl. Acad. Sci. U.S.A.*, **73**, 1384 (1976). (b) W. E. Blumberg, J. Peisach, and L. Powers, manuscript in preparation.
- (46) E. B. Fleischer, C. K. Miller, and L. E. Webb, *J. Am. Chem. Soc.*, **86**, 2342 (1964).
- (47) P. H. Citrin, P. Eisenberger, and B. M. Kincaid, *Phys. Rev. Lett.*, **36**, 1346 (1976).
- (48) B. K. Teo, P. A. Lee, A. R. Simons, P. Eisenberger, and B. M. Kincaid, *J. Am. Chem. Soc.*, **99**, 3854 (1977).
- (49) L. Vaska, *Acc. Chem. Res.*, **9**, 175 (1976).
- (50) W. P. Schaefer, *Inorg. Chem.*, **7**, 725 (1968).
- (51) R. S. Himmelwright, N. C. Eickman, and E. I. Solomon, *Biochem. Biophys. Res. Commun.*, **88**, 628 (1979).
- (52) M. Cannas, A. Cristini, and G. Marongiu, *Inorg. Chim. Acta*, **19**, 241 (1976).
- (53) (a) P. E. Eller and E. W. R. Corfield, *Chem. Commun.*, 105 (1971). (b) D. F. Lewis, S. J. Lippard, and P. S. Welcker, *J. Am. Chem. Soc.*, **92**, 3805 (1970). (c) A. H. Lewin, R. J. Michl, P. Geddes, and U. Lappour, *J. Chem. Soc., Chem. Commun.*, 661 (1972). (d) D. M. S. Weininger, G. W. Hunt, and E. L. Amma, *ibid.*, 1140 (1972).
- (54) R. S. Himmelwright, N. C. Eickman, and E. I. Solomon, *Biochem. Biophys. Res. Commun.*, **81**, 237 (1978).
- (55) R. S. Himmelwright, N. C. Eickman, and E. I. Solomon, *Biochem. Biophys. Res. Commun.*, **81**, 243 (1978); **84**, 300 (1978); *J. Am. Chem. Soc.*, **101**, 1576 (1979).
- (56) T. J. Thaman, J. S. Loehr, and T. M. Loehr, *J. Am. Chem. Soc.*, **99**, 4187 (1977).
- (57) D. M. Kurtz, D. F. Shriver, and I. M. Klotz, *J. Am. Chem. Soc.*, **98**, 5033 (1976).
- (58) W. B. Pearson, "Lattice Spacings in Metals and Alloys", Pergamon Press, London, 1957.
- (59) J. N. van Niekirk and R. R. L. Schoening, *Acta Crystallogr.*, **6**, 227 (1953).